Desalination and Water Treatment
www.deswater.com

doi:10.5004/dwt.2017.21554

94 (2017) 198–210
October

Adsorption of copper(II) and zinc(II) ions from aqueous solution by activated carbon derived from halophytes (*Suaeda maritime*)

Mohamed M. El-Bouraie[a,*], Gehad G. Mohamed[b]

[a]*Chemistry Department, Central Laboratory for Environmental Quality Monitoring (CLEQM), National Water Research Center (NWRC), El-Qanater El-Khairiya P.B.13621, Egypt, Tel. +201221839311, Email: mido.chemie@gmail.com*
[b]*Chemistry Department, Faculty of Science, Cairo University, Egypt, Email: ggenidy68@hotmail.com*

Received 18 March 2017; Accepted 15 October 2017

ABSTRACT

Sample of a halophytes activated carbon (ACHs), *Suaeda maritime*, has been carbonized after impregnating with H_3PO_4. Batch adsorption technique was employed for the metal ions biosorption onto ACH2 in a single component system. The activated carbon prepared was characterized by SEM, XRD, FTIR analysis and also ash content, bulk density, moisture content, BET surface area and porosity analysis, were carried out. The influence of pH, contact time, initial metal ions concentration and temperature on metal sorption capacity have been examined. The maximum sorption capacities calculated by applying the Langmuir isotherm were 29.41 mg/g for Cu, and 14.64 mg/g for Zn, respectively. Thermodynamics and kinetic adsorption of two metal ions were examined in batch experiments. It was verified that the Freundlich, Langmuir and Temkin isotherms describe the adsorption of Cu(II) and Zn(II) ions reasonably well. Adsorption of Cu(II) and Zn(II) ions onto ACH2 was better fitted to Freundlich isotherm model. According to the obtained thermodynamic data, the adsorption of Cu(II) and Zn(II) ions onto ACH2 were spontaneous and an endothermic processes with large adsorption enthalpy. The kinetic study showed that the whole adsorption process fit the pseudo-second-order kinetics model well. The kinetic data confirmed that particle diffusion is not the only rate-limiting step in the adsorption process.

Keywords: Halophytes; Sorption; Batch adsorption; Activated carbon; Thermodynamics

1. Introduction

Heavy metals such as copper and zinc are among the most toxic and easily encountered metals released into the environment through various industrial activities, consumer products, and waste disposal [1]. As such, they are stable elements and can't be degraded biologically by the body. They can be passed into the food chain to humans via wastewater from industrial and domestic activities. Heavy metals are taken into the body via inhalation, ingestion, and skin absorption. Heavy metal pollution may be occurred due to irrigation with contaminated water, the addition of fertilizers and metal-based pesticides, industrial emissions and transportation. Food and agriculture organization (FAO) recommended the maximum acceptable concentration of copper and zinc in irrigation water as 0.2 and 2.0 mg L^{-1}, respectively [2,3].

Several technologies were available to remediate heavy metals pollution. However, many of these technologies were costly or not achieve a long-term nor an aesthetic solution [4,5]. Till now, treatment of industrial effluents containing heavy metals as copper and zinc is mainly based on precipitation, coagulation, ion exchange, membrane filtration and electroplating. These processes are usually expensive and sometimes ineffective, especially when the concentration of heavy metals is low [6]. Adsorption had been investigated as an efficient technique for the removal of heavy metals from wastewater. Among these methods, carbon adsorption was the most widely used absorbent materials because of its simplicity and economic feasibility. It has also been shown that adsorption is one of the most effective removal

*Corresponding author.

methods for the aqueous solution containing low concentration heavy metal.

Recently, activated carbon with a high surface area and porosity may be obtained as the precursor then activated in the presence of air and phosphoric acid at moderate temperatures. Activated carbon obtained by this procedure was shown to have a high capacity towards the removal of copper and zinc from aqueous solutions compared to that of commercial materials [7–10]. This large capacity was associated with the existence of functional groups on the surface.

Halophytes are of significant interest since these plants are naturally present in environments with an excess of toxic ions and research findings suggested that these plants also tolerate other environmental stresses, especially heavy metals as their tolerance to salt and heavy metals may, at least partly, rely on common physiological mechanisms [11]. They play an important role in protecting habitats and maintaining ecological stability. Halophytes also have huge potential to aid agricultural development and habitat restoration in areas affected by salinity.

The main objective of the present study was an investigation of the adsorption characteristics of Cu(II) and Zn(II) onto halophytes (*Suaeda maritime*) activated carbon in a single component system. Physical and chemical characterizations of these materials were carried out to examine the relationship between their sorptive, physical and chemical properties. These studies consisted of porosity, BET surface area, scanning electron micrographs (SEM), Fourier transform infra-red spectroscopy (FTIR) analysis, zeta potential measurements and pH titration were used to understand the adsorption mechanism. The effects of pH, contact time, activated carbons derived from halophytes (ACH) dose, initial Cu(II) and Zn(II) concentration and temperature on the adsorption of Cu(II) and Zn(II) from aqueous solutions were studied the adsorption characteristics including the sorption capacity, thermo-dynamics, kinetics, and adsorption isotherm of ACH were also investigated. These results are valuable for further application of ACH in the adsorption of Cu(II) and Zn(II) from aqueous solutions.

2. Materials and methods

2.1. Preparation of solutions

All chemicals utilized in this study were of analytical grade and supplied by Merck, (Germany). Stocks solutions of copper(II) and zinc(II) ions (1000 mg/L) were prepared by dissolving (1.965 g) $CuSO_4{\cdot}5H_2O$ and (2.199 g) $ZnSO_4{\cdot}7H_2O$ in 500 mL of deionised water then diluted to different concentration. Solution pH was adjusted with 0.1 M NaOH and 0.1 M HCl solutions and measured by using a pH meter (WTW pH meter, Model 3110). The concentration of copper(II) and zinc(II) ions in the aqueous solution after adsorption was determined by an inductively coupled plasma optical emission spectrometry (ICP-OES; PerkinElmer Optima 7000 DV, USA).

2.2. Activated carbon preparation

Halophytes (*Suaeda maritime*) were collected from Mediterranean coastal salt marsh region in New Damietta, Egypt. Prior to use, samples were washed gently with water to remove sand dunes, mudfats and other impurities present on the surface and then dried in oven at 120°C for 24 h or until constant weight to reduce moisture content. All plant parts were weighed to determine the dry weight and then were smashed into plant powder. The samples were weighed to determine the dry weight and then were smashed into plant powder. 50 g of ACHs was impregnated with 200 mL of 20%, 40%, 60% and 80% w/v H_3PO_4 solution and soaked for 4 h under anaerobic condition; then the mixture was stirred at 85°C for 1 h to the interior of the precursor. After impregnation, the material was carbonized under closed conditions. The temperature was raised at 4°C/min to 500°C, which was maintained for 3 h. The samples were cooled and then washed to remove excess reagent. The mixture was then subjected to heat at a temperature of 120°C for 3 h to vaporize the water. The dried mixture was subjected to heat at a temperature of 650°C in a muffle furnace to enable activation of the pores of the carbon sample. The dried biomass (ACHs) was preserved in air-tight glass bottles to protect it from moisture.

2.3. Characterization of activated carbon

All adsorption experiments were carried out on a thermostated shaker (THZ-82, Guohua apparatus company, China) operated at 200 rpm. The impregnated ACH samples were analyzed by scanning electron microscopy (SEM; JSM 6390LV, JEOL: Japan), Fourier transform infrared spectrophotometry (FTIR) (Perkin-Elmer 1720 spectrometer), the surface area and porosity were performed by N_2 adsorption at –196°C using the BET method on a Micromeristic ASAP 2000, USA instrument. The zeta potential measurement of ACHs samples was calculated using the Henry equation (Zetasizer Nano ZS equipped with an autotitrator – Malvern Instruments Ltd., UK). The concentrations of metal ions were measured on an inductively coupled plasma optical emission spectrometry (ICP-OES; PerkinElmer Optima 7000 DV, USA).

2.4. Batch adsorption experiments

Adsorption experiments were performed by using the batch technique to acquire the rate and the equilibrium data. Influence of value of pH, adsorption time, initial concentration of Cu(II) or Zn(II) in a single system, ACH2 dosage, and temperature: 250 mL conical flasks containing 50 mL of Cu(II) or Zn(II) solution of desired concentration mixed with 0.01–0.15 g ACH2 were agitated in a shaker with 200 rpm for different adsorption time at specified temperature and pH value. The initial pH of the solution was regulated by 1 M NaOH and HCl solutions detected by a pH meter. The contact time varied from 1 to 240 min. The temperature and pH ranged from 20 to 50°C and 2 to 8, respectively. After shaken in the oscillator, the content of Cu(II) and Zn(II) in the mixed liquor after filtrated was measured by ICP-OES. For copper, Adsorption studies were carried out by using 0.07 g ACH2 with the initial concentration of Cu(II) from 5 to 300 mgL^{-1}. The mixture was vibrated at 200 rpm for 90 min at pH 6. On the other hand, Adsorption experiments

were conducted for zinc by using 0.06 g ACH2 with the initial concentration of Zn(II) from 5 to 300 mg/L. The mixture was vibrated at 200 rpm for 120 min at pH 5. Adsorption kinetics experiments were conducted by using 0.07 and 0.06 g ACH2 with 5 to 25 mg L^{-1} for Cu(II) and 1 to 150 mg L^{-1} for Zn(II) at pH 6 and 5, respectively. The mixture was shaken at 200 rpm at 25°C and the contact time varied from 1 to180 min. In a single system, the batch experiments for adsorption thermodynamics of Cu(II) or Zn(II) were carried out at varying temperatures (293, 298, 303, 308, 313, 318 and 323 K) with different initial concentrations. Each determination in the batch adsorption experiment was carried out in triplicate, and repeated at least twice; the results are given as average values. Error bars are also indicated wherever necessary.

From the measured concentrations of Cu(II) and Zn(II) ions, the amount of metal ion adsorbed, q_t (mg/g) was computed by the following equation.

$$q_t = (C_i - C_t)V / W \quad (1)$$

The removal efficiency of metal ion was also calculated by using Eq. (2).

$$R\% = \frac{(C_i - C_t)}{C_i} \times 100 \quad (2)$$

where, q_t: is the adsorption capacity at time t (mg g^{-1}), $R\%$ is the removal efficiency of metal ions adsorbed, C_i and C_t are metal concentrations (mg L^{-1}) before and after adsorption, V is the volume of adsorbate (L) and W is the weight of the adsorbent (g).

2.5. Adsorption kinetics

Kinetic models were used to determine the rate of the adsorption process besides providing valuable information about reaction pathways. In this context, the kinetics of the adsorption of Cu(II) and Zn(II) ions were also evaluated. The kinetics of an adsorption process describes the mechanism of adsorption depends on the physical and chemical characteristics of the adsorbents. The kinetic models of Lagergren pseudo-first-order, pseudo-second-order, Elovich equation, and Intraparticle diffusion Weber-Morris model were investigated to understand the adsorption dynamics of each on Cu(II) and Zn(II) on ACH2. All kinetic models were fit to experimental data using their linear equations which are shown in Table 1.

2.6. Equilibrium adsorption isotherm

To describe experimental results, the linear form of Langmuir, Freundlich and Temkin isotherm equations were applied to determine the effect of presence of metal ions adsorbed on the isotherm constants. Recent studies also used the Langmuir and Freundlich models to fit the experimental data for adsorption of Cu(II) and Zn(II) ions onto activated carbon in a single system [1,10].

The Langmuir model was based on the assumption that maximum adsorption correspond to a saturated monolayer of solute molecules on the adsorbent surface, with no lateral interaction between the adsorbed molecules. The linear form of the Langmuir isotherm model was given by applying Eq. (3):

Table 1
The linear equations of kinetic models.

Kinetic models	Equation
Pseudo-first-order	$\log(q_e - q_t) = \log(q_e) - \frac{k_1}{2.303}t$
Pseudo-second-order	$\frac{t}{q_t} = \frac{1}{k_2 q_e^2} + \frac{t}{q_e}$
Elovich	$q_t = \frac{1}{\beta}\ln(\alpha\beta) + \frac{1}{\beta}\ln t$
Intraparticle diffusion Weber-Morris	$q_t = k_d t^{1/2} + C$

$$\frac{C_e}{q_e} = \frac{1}{q_m K_a} + \frac{C_e}{q_m} \quad (3)$$

where, q_e (mg g^{-1}) is the amount of equilibrium uptake, C_e is the equilibrium cation concentration in solution (mg L^{-1}), q_m is the monolayer adsorption capacity of the adsorbent (mg g^{-1}), and K_a is the Langmuir adsorption constant (L mg^{-1}), which is related to the rate of adsorption. The Langmuir constants q_m and K_a can be calculated from the slope and intercept of the linear plot of C_e/q_e vs. C_e.

The effect of isotherm shape on the favorability of a Langmuir-type adsorption process can also be expressed in terms of a dimensionless constant separation factor or equilibrium parameter, R_L, which can be calculated by using Eq. (4):

$$R_L = \frac{1}{1 + K_a C_o} \quad (4)$$

where K_a is the Langmuir isotherm constant and C_o is the initial concentration of Cu(II) ions. The value of R_L indicates the isotherm to be either unfavorable ($R_L > 1$), linear ($R_L = 1$), favorable ($0 < R_L < 1$), or irreversible ($R_L = 0$).

The Freundlich isotherm was applied for non-ideal adsorption on heterogeneous surfaces and multilayer adsorption. The Freundlich isotherm can be written in linear form as given below Eq. (5):

$$\log q_e = \log K_f + \frac{1}{n}\log C_e \quad (5)$$

where K_f and n are Freundlich constants, with K_f (mg g^{-1}) being the adsorption capacity of the adsorbent and n giving an indication the favorability of the adsorption process. Values of $n > 1$ represent favorable adsorption conditions. The Freundlich constants k and n can be calculated from the slope and intercept of the linear plot of log q_e versus log C_e.

The Temkin isotherm described that the binding energy decreased linearly with increasing amounts of metals bound to the surface due to adsorbent-adsorbate interactions [12].

The Temkin isotherm can be expressed in its linear form by the following Eq. (6):

$$q_e = B_t \ln\ln K_t + B_t \ln\ln C_e \quad (6)$$

where $B_T = (RT/b_T)$ is Temkin constant related to the heat of adsorption (kJ mol^{-1}), T is the absolute temperature (K), R is the universal gas constant (8.314 J mol^{-1} K^{-1}), K_T is the equilibrium binding constant (L mg^{-1}), and b_T is the variation of adsorption energy (kJ mol^{-1}). The Temkin constants for the two metal ions are determined by plotting q_e against ln C_e.

3. Results and discussion

3.1. Physical characterization

The data of impregnation with different ratio H_3PO_4 solution, bulk density, moisture, ash content, BET surface area and porosity of ACHs are shown in Table 2.

Moisture and dry matter percentage of activated carbon derived from Halophytes (*Suaeda maritime*) increased with increasing salinity of the growing medium. This attributed to a simple hypertrophy resulting from the increased osmotic pressure. From Table 1, there is no correlation between effect of impregnation ratio and percentage of moisture and dry matter [13].

Bulk density was an important characteristic of the carbon and was invariably related to the starting material [14]. In this study, high value of bulk density may be as a result of its hydrophilic nature. Ash was non-carbon or mineral additives, which was not chemically combined with the carbon surface. It consists of various useless mineral substances, which become more concentrate during the activation process. It comprises of 1–20% and primarily depends on the type of raw material. Low ash content with increasing concentration of H_3PO_4 is desirable for activated carbon (ACH2), since it reduces the mechanical strength of carbon and affects adsorptive capacity [15].

Fig. 1 shows the N_2 adsorption-desorption isotherms of ACH2 prepared by phosphoric acid activation. According to the BET analysis, the isotherm exhibit a Type IV profile according to the IUPAC classification, with displays the H3 hysteresis loop in relative pressure higher than 0.8. The hysteresis loop of this isotherm is associated with filling and emptying of the mesopores by capillary condensation. The type H3 loop, which does not exhibit any limiting adsorption at high P/P_0, is adsorbed with aggregates of plate-like particles giving rise to slit-shaped pores [16]. As seen in Fig. 1, there is nonsignificant uptake of nitrogen at lower relative pressure (P/P_0), indicating that there are few micropores in ACH2. It can be noted that the increasing in a BET surface area and porosity of ACH2 with temperature can be attributed to the impregnated with phosphoric acid [17]. It is found that BET surface area and porosity are obtained for ACHs samples, as tabulated in Table 2. The results are consistent with the findings of other workers [18], suggested that increasing the amount of phosphorus leads to an increase in the volumes of macro- and mesopores.

Fig. 2 shows zeta potential of activated carbon samples as a function of equilibrium pH for ACH1, ACH2, ACH3 and ACH4. Zeta potential is an important parameter to characterize electrokinetic behavior of solid-liquid interface. Zero point charge (pHpzc) was taken as the point where zeta potential was zero and it reflects the character of external surface of activated carbon particles. The analysis of the test results shown in Fig. 2, indicates that the electrokinetic potential of ACH samples change in the research conditions from +10.45 to –17.56 mV and the Zero point charge can be interpolated to be about 4.6 pH. This means that external surface of activated carbon samples has positively charged when pH was less than 4.6 [19,20]. After this point, zeta potential decreases markedly. Negative zeta potential of ACH samples can be attributed to the negative charge of organic functional groups resulting from the dissociation of H^+ ions although it has been carbonized at very high temperatures according to the following reaction:

$$R\text{-}COOH \leftrightarrow R\text{-}COO^- + H^+$$

Table 2
Physical parameters of ACHs samples

Parameters	Samples			
	ACH1	ACH2	ACH3	ACH4
Impregnation with H_3PO_4(%)	20	40	60	80
Moisture content (%)	8.5	8.0	8.9	9.4
Dry matter (%)	82.4	82.1	80.86	80.1
Bulk density (g/L)	459	464	469	472
Volatile matter (%)	6.2	6.7	6.9	7
Ash content (%)	2.9	3.2	3.34	3.5
Porosity (cc/g)	0.857	0.874	0.865	0.842
BET Surface area (m^2/g)	978	987	991	1021
pH_{PZC}	4.8	4.6	4.7	4.8

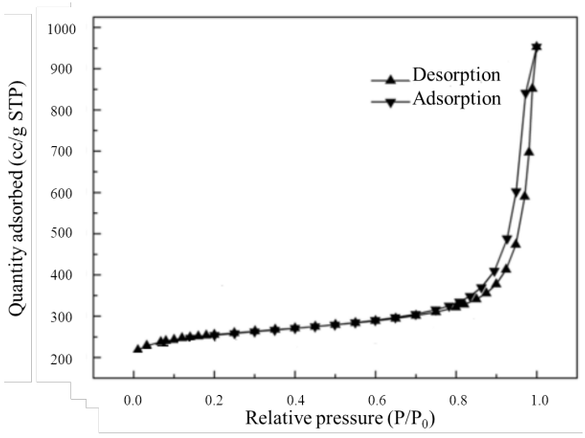

Fig. 1. Nitrogen adsorption-desorption isotherm of activated carbon.

4. Chemical characterization

4.1. FT-IR Analysis of ACH

The FT-IR spectra can be established to identify the functional groups present in activated carbon before and

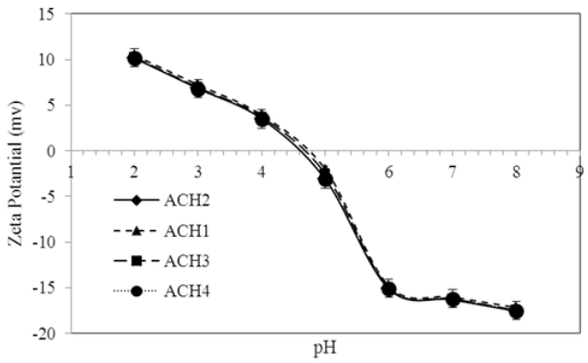

Fig. 2. The zeta potential (ZP) of ACH samples in the pH range 2–9.

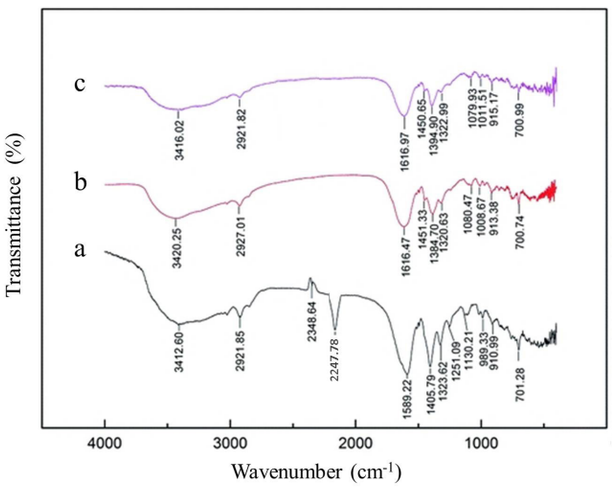

Fig. 3. The FTIR spectra of activated sample of Halophytes before adsorption (a), after adsorption of Cu(II) (b) and Zn(II) (c).

after adsorption of copper and zinc as shown in Fig. 3a, 3b, 3c and 3d, respectively. Functional groups of adsorbents are not only affect the adsorption behavior, but also dominate the adsorption mechanism [21]. The (–OH), (–NH), carbonyl and carboxylic groups are important sorption sites. The peak at 3412 cm^{-1} is attributed to –OH and –NH groups. The band between 3000–3500 cm^{-1} has been assigned to –OH stretching vibration of hydroxyl groups. These bonds are present in activated sample and metal loaded adsorbents; indicating participation of the (O–H) functional group in the metal binding. The intensity of –OH is weakened after adsorption process. The –OH peak at 3412 cm^{-1} is slightly shifted to 3420 cm^{-1} (at copper adsorption) and 3416 cm^{-1} (at zinc adsorption). The band at 1589 cm^{-1} is the C=O symmetric stretching vibration of carboxylic acid groups in the biosorbent; the peak at 2921 cm^{-1} is attributed to the symmetric and asymmetric C–H stretching vibration of $–CH_2$ and $–CH_3$ groups; 2348 cm^{-1} attributed the characteristic peak of $–NH_2$. The presence of –OH group, coupled to carbonyl group confirmed the presence of carboxylic acid groups in the biosorbent [22]. After biosorption, the intensity of –OH is weakened; the –OH peak at 3412 cm^{-1} is slightly shifted to 3420 cm^{-1} (at copper adsorption) and 3416 cm^{-1} (at zinc adsorption).The C=O peak was shifted from 1589 cm^{-1} (activated carbon) to 1616 cm^{-1} (copper adsorbed) and 1616 cm^{-1} (zinc adsorbed). The intensity of C=O is weakened after loading with copper and so with zinc. These findings suggest that the hydrogen and oxygen atoms in the –OH and were involved in the copper and zinc adsorption. The metal loaded on ACH may form coordinate covalent bond with –COOH. After metal loading, the peak of $–NH_2$ at 2348 cm^{-1} is disappeared. These results indicate that $–NH_2$ may be involved with the adsorption process as well as the metal loading process. The schema of the listed forms of complexes is shown in Fig. 3. Transition metals can form complexes with carboxylate in three forms, which are monodentate complexes, bidentate complexes and bridge complexes.

This indicate the participation of hydroxyl and carbonyl groups in the biosorption of copper(II) and zinc(II) ions. Similar spectra are obtained for biosorption studies of metal ions using groundnut hull [22], and palm nut shells [23]. The sharp band at 2247 cm^{-1} appears to the functional group of phosphorus belonging to phosphine (P-H). At 989 cm^{-1}, the peak is associated with P-O-C carbons asymmetric stretching. This is proven in the study of that acid phosphates form in the samples modified using H_3PO_4. The broad band in this range is due to the presence of phosphorous compounds in the samples [15]. The bands in the interval 1000–1320 cm^{-1} have been indicated to C–O stretching in acids, alcohols, phenols, and esters [18,24]. Due to the overlap of adsorption bands from various oxygen and phosphorous compounds in this region. It seems that steam activation of samples impregnated with H_3PO_4 leads to decomposition of the phosphoric compounds. The adsorption at 1300–900 cm^{-1} with the peak at 1320–1080 cm^{-1} was tentatively assigned to the following phosphorous species as in Fig. 3b and c: hydrogen-bonded P=O, O–C stretching vibrations in P–O–C of aromatics and P=OOH [25,26]. In the present study, the increase of the negative charge of phosphate groups on ACH surface led to thus adsorption ability for Cu(II) or Zn(II) ions increased [1].

The peaks of N–H and C=O (ester stretching) bands disappeared in metal-loaded adsorbent may be due to the destruction of the functional group during the process of adsorption but appeared after activation.

4.2. SEM Analysis of ACH

To study the effect of activation on porosity, Scanning Electron Microscope (SEM) technique is employed to observe the surface physical morphology of the biosorbents before and after metal ion adsorption. The SEM images for activated Halophytes before and after metal interaction are shown in Fig. 4. SEM analysis revealed that there are significant changes on the surface of biosorbents after interaction with metal ions. The SEM analysis confirmed that the morphological structure of activated Halophytes is porous in nature. A possible explanation for this was that cellulosic materials of biological origin have systems of interconnecting pores, thus providing a relatively high surface area [27]. From Fig. 4a, the surface structures of the ACHs have a cleaner and burnout pores with a tunnel or honeycomb-like structures, which are suitable for copper and zinc ions to be adsorbed on the surface and

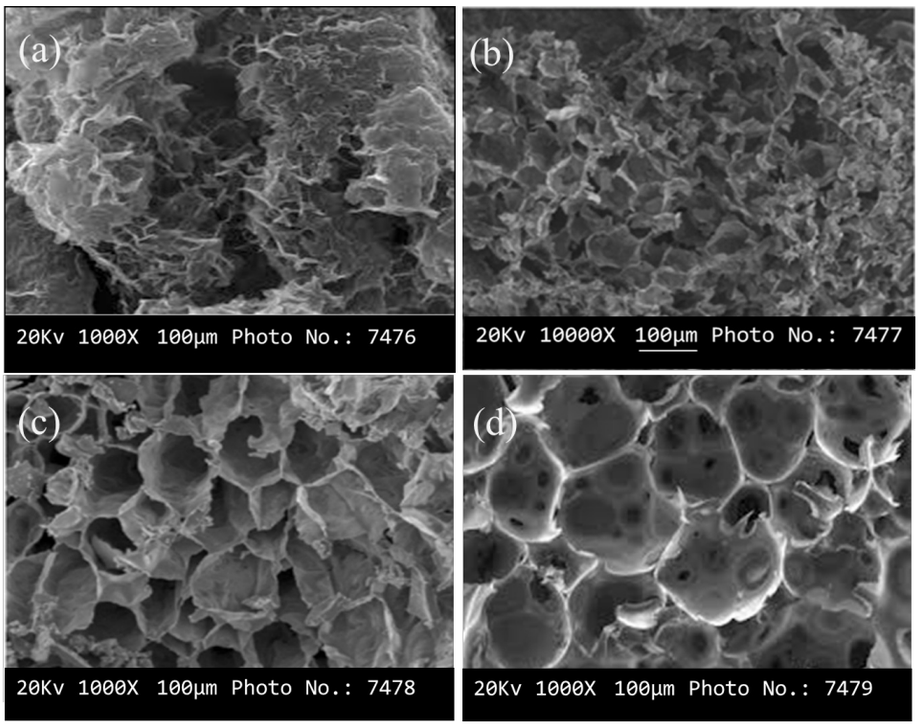

Fig. 4. SEM images of ACH before (a), after activation by H_3PO_4 (b) then adsorption of Cu(II) (c) and Zn(II) (d) at magnification of 1000×.

these results are in good agreement with XRD analyses. Fig. 4b shows the differences of the surface and porosity of the activated carbon prepared (ACH2) at 40 wt.% H_3PO_4. It is obvious that the carbons produced at 40 wt.% have cavities and cracks on their external surfaces. It seems that the cavities on the surfaces of carbons resulted from the evaporation of phosphoric acid during thermal treatment, leaving the space previously occupied by the impregnation agent. After interaction with Cu(II) ion, the surface of ACH2 became irregular. Flakes-like deposits were observed on the surface of ACH2 following interaction with Cu(II) ions as in Fig. 4c and 4d, whereas the surface structures of the ACH have Lump- and twist-like deposits were observed on the surface with Zn(II) ions.

4.3. X-ray diffraction analysis of ACH

The X-ray diffraction (XRD) analysis was carried out to study changes in the microstructures of ACHs and metal ion-adsorbed carbon as shown in Fig. 5a, b and c, respectively. The intense main peak showed the presence of highly organized crystalline structure of raw activated carbon. The diffraction peak of crystalline carbon is observed, where broad diffused peaks are observed at low angles. After the adsorption of metal ion, the intensity of the highly organized peaks are slightly diminished. This has attributed to the adsorption of metal ion on the upper layer of the crystalline structure of the carbon surface by means of chemisorption rather than physisorption. The features of Cu(II) ion appeared at 40.93 and 49.24 degree. Interaction with Zn(II) had caused the appearance of Zn(II) feature at 59.67 degree.

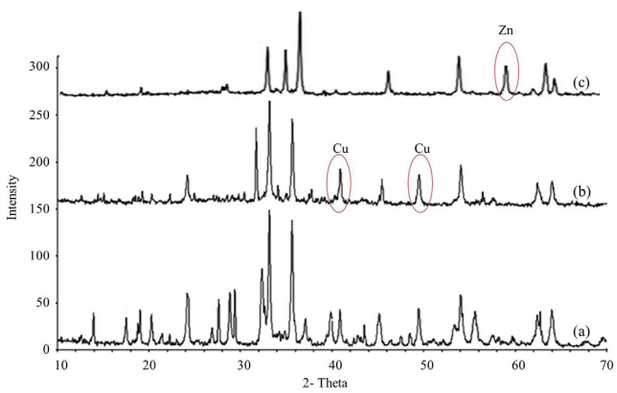

Fig. 5. XRD spectrum of activated sample of Halophytes before adsorption (a), after adsorption of Cu(II) (b) and Zn(II) (c).

The X-ray diffraction peak confirmed that ACH2 possesses a heterogeneous surface.

4.4. Equilibrium studies on biosorption of Cu(II) and Zn(II) ions Effect of pH

In the first stage of the study, the pH value of the heavy metal solution plays a major role in the adsorption process. Fig. 6, showed the effect of pH value on metal ion uptake onto ACH2. The influence of pH on the adsorption capacity of ACH2 was studied over the 2.0–6.0 pH range in the single-metal system, and the results are shown in

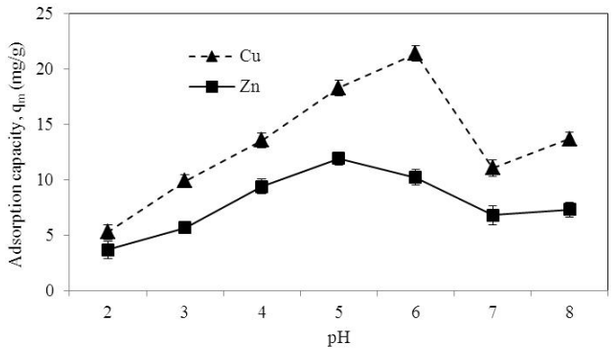

Fig. 6. Effect of pH on Cu(II) and Zn(II) adsorption capacity by ACH2 (metal ion concentration 5–300 mg/L, adsorbent dose 0.06–0.07 g, volume of sample 50 mL, time 1–240 min).

Fig. 6. Generally, the interaction mechanisms between both metal ions and biosorbent were function of pH that involved physisorption. Therefore, the optimum pH for the removal of Cu(II) and Zn(II) ions by using ACH2 were recorded at pH 6.0 and 5.0, respectively, and the subsequent experiments were carried out at this pH value. The maximum adsorption of Cu(II) and Zn(II) ions onto adsorbent increased from 5.32 to 21.42 and 3.71 to 11.94 mg g^{-1}, respectively. When the pH value was greater than 7.0, it was likely that both metal ions were precipitated as a result of the formation of hydroxides. Therefore, the removal of metal ions at higher pH values was due to the formation of precipitates (Chemsisorption) rather than adsorption. At lower pH values, H_3O^+ ion exist in high concentration and binding sites of metals became positively charged and this has a repelling effect on both metal ions. As the pH value increased, the concentration of H_3O^+ ion in the solution decreased, lowering the competition of metal ion for active sites, hence increasing metal uptake. This was in good agreement with the previous explanations [28]. The decrease in removal of both metal ions at pH greater than 6.0 may be due to solvation and hydrolysis of metal ion [29]. The solvation and hydrolysis process lead the metal ion to form soluble hydroxylated complexes that compete for active sites. Moreover, the nature of ionization on the surface of biosorbents at specific pH may also cause the reduction of metal ions removal (chemisorption), as shown in the following reactions (Fig. 7).

Where R– represents the surface sites of activated carbon; $R–OH_2^+$, R–OH, $R–O^-$ represent protonated, neutral, and ionized surface hydroxyl functional groups; $R–OM^+$ and R–OM(OH) were formation of the bonding complexes. It can be seen that at low pH values, H competes with the Cu(II) ions for the active surface sites and, moreover, the less functional groups, i.e. $R–O^-$ were ionized (deprotonated) in this region, and it was difficult that they formed metal complexes. Noted here M^{2+} and $M(OH)^+$ were the dominant species involved in the adsorption below pH 6.0, thus other species $M(OH)_2$ and $M(OH)^{3-}$ weren't accounted in the formation of surface complexes (Reddy et al., 2010). The adsorption capacity of Cu(II) ion was higher than Zn(II), may be due to the fact that Cu(II) has a smaller ionic radius than that of Zn(II) and can exchange with H^+ more easily [30]. The pH_{PZC} value is the point at which surface functional groups do not contribute to the pH of the solution. The activated carbons produced are effective adsorbents for removing Cu(II) and Zn (II) ions at pH ≥ pH_{PZC}. The pH_{PZC} value determined for ACH indicate their acid nature, which was expected due to the treatment applied to the carbons, which caused the introduction of oxygenated groups [31]. As regards the distribution of acid sites, the number of carboxylic groups was larger in carbons ACH, which also had the smaller acid pH_{PZC} values, since these groups correspond to higher strength acids. Activated carbon produced from halophytes (ACH2) has a higher content had a higher content of carboxylic functional groups and its pH_{PZC} was 4.6 as shown in Fig. 3.

$$R\text{-}OH_2^+ \longleftrightarrow R\text{-}OH + H^+ \quad \text{(i)}$$
$$R\text{-}OH \longleftrightarrow R\text{-}O^- + H^+ \quad \text{(ii)}$$
$$R\text{-}O^- + M^{+2} \longleftrightarrow R\text{-}OM^+ \quad \text{(iii)}$$
$$R\text{-}O^- + M(OH)^+ \longleftrightarrow R\text{-}OM(OH) \quad \text{(iv)}$$

Fig. 7. The adsorption mechanism for Cu(II) and Zn(II) ions onto ACH2.

4.5. Effect of contact time

The change of adsorption capacity of ACH2 with contact time of Cu(II) and Zn(II) is shown in Fig. 8. The results show that a state of equilibrium of the adsorption of Cu(II) and Zn(II) increased with contact time from 10–50 min. Within the first 30 min, metal adsorption was rapid and reducing gradually over time until equilibrium was conducted at a contact time of 80 min for Zn(II) and 100 min for Cu(II) because of the availability of a large number of adsorbent sites during the initial stages of the process. The occupation of active sites on the surface of ACH2 by adsorbates is a gradual process in solution, which requires certain time to reach equilibrium adsorption [32]. The fast adsorption is probably due to the relatively high specific surface area and more functional groups like hydroxyl groups, carboxylic groups, carboxylate moieties, and phosphate groups presented on ACH2. The results revealed that, the maximum adsorption of Zn(II) ions was lower than for Cu(II) ions. This attributed to the electronegativity of Cu(II) and Zn(II) ions are 1.90 and 1.65 (Pauling scale), respectively; thus, the greater electronegativity of Cu(II) may enhance the binding capacity of copper toward the negatively charged adsorbent surface, resulting in a slightly higher adsorption capacity for Cu(II) than Zn(II) ions [33].

4.6. Effect of adsorbent amount and initial concentration of metal ions

The changes of adsorption capacity of ACH2 with adsorbent dose and initial solution concentrations of Cu(II) and Zn(II) are shown in Figs. 9 and 10. The results also showed that,the adsorption capacity of Cu(II) and Zn(II) (broken line in Fig. 9) by ACH2 descended from 21.47 to 1.49and from 34.52 mg g^{-1} to 1.26 mg g^{-1}, respectively, when the ACH2 dosage enhanced from 0.01 to 0.15 g. On the other hand,the percentage removal of Cu(II) and

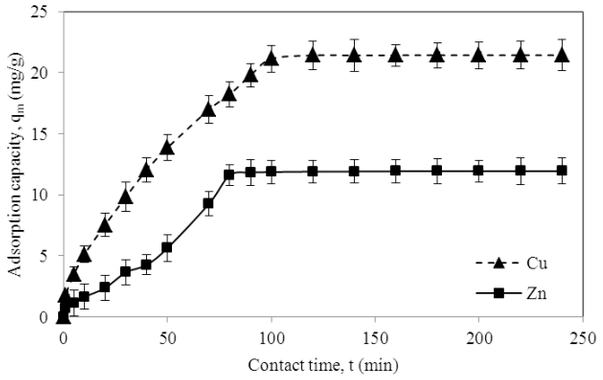

Fig. 8. Effect of contact time on the removal of Cu(II) and Zn(II) ions by ACH2.

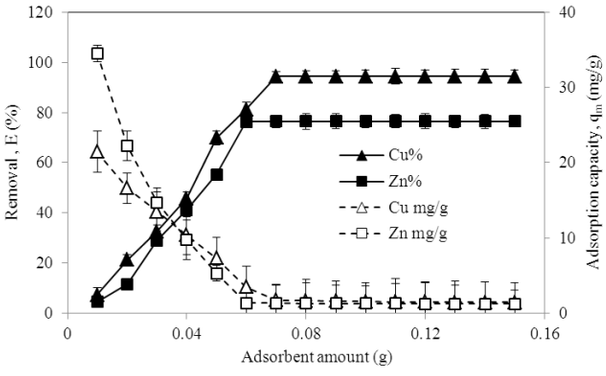

Fig. 9. Effect of adsorption amount on removal efficiency and adsorption capacity by ACH2.

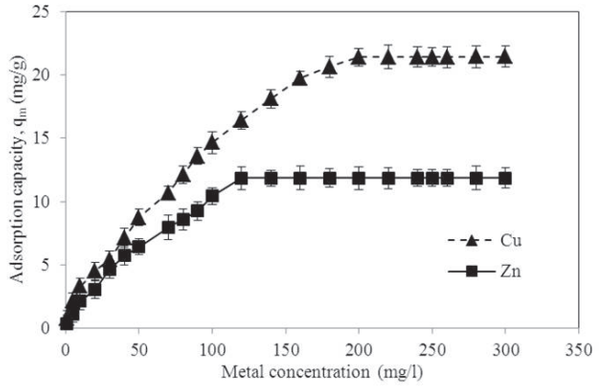

Fig. 10. Effect of metal ions concentration on adsorption capacity by ACH2.

Zn(II) (line in Fig. 9) increased fast from 7.46 to 69.96% and from 4.57 to 55.37%, respectively, with the increasing doses of ACH2 from 0.01 to 0.05 g, and reached up to 94.31 and 76.42%, respectively, when the ACH2 dosage is 0.15 g. In the present study, the Cu(II) and Zn(II) adsorption onto ACH2 was significantly affected by the original content concentration of Cu(II) and Zn(II). The adsorption amount

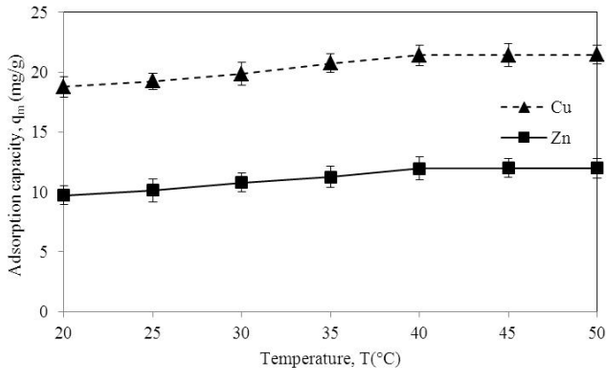

Fig. 11. Effect of temperature on Cu(II) and Zn(II) adsorption capacity by ACH2.

of Cu(II) and Zn(II) by ACH2 increased from 2.17 to 21.42 mg g^{-1} and from 1.11 to 11.87 mg g^{-1}, respectively, with the increase of initial concentration of Cu(II) and Zn(II) from 5 to 300 mg L^{-1}. This can also be illustrated in terms of high adsorption at low metal concentrations can be attributed to availability of vacant sites for metal binding [34]. In contrast, at high metal concentrations the active sites of adsorbents were less available, reducing metal ion removal. It can be concluded that adsorption of metal ions from aqueous solutions increased with increasing atomic weight and ionic radii.

4.7. Effect of temperature

The effect of temperature on adsorption of Cu(II) and Zn(II) onto ACH2 was studied at temperature range of 20–50°C. The adsorption capacity of both metals onto ACH2 increased as temperature increased from 20 to 40°C indicating an endothermic adsorption process as shown in Fig. 11. It is observed that, the effect of temperature on Zn(II) adsorption onto ACH2 was more apparent than that of Cu(II). There was no appreciable increase in adsorption amount for both metal ions from 40 to 50°C, indicating that ACH2 is suitable for heavy metal removal in wastewater. Hence, the result suggested that 40°C as adsorption temperature in this experiment had a greater effect on the adsorption process implying that the surface coverage increased at higher temperatures. This may be attributed to the increased penetration of metal ions inside micropores or the creation of new active sites at higher temperatures [35]. This indicated the endothermic nature of the controlled adsorption process. Thermodynamic parameters of ΔS°, ΔH°, and ΔG° were calculated and were listed in Table 3. ΔH° and ΔS° can be deduced from Fig. 12. The negative values of Gibbs free energy change (ΔG°) confirmed that the adsorption of Cu(II) and Zn(II) ions onto ACH2 was spontaneous, and the incline of ΔG° as a function of temperature indicated that temperature helps to the adsorption procession [36]. The positive ΔH° values indicated that the adsorption of Cu(II) and Zn(II) ions on ACH2 was an endothermic process. The increasing positive value of ΔS° probably indicated the enhanced adsorption randomness at the solid liquid interface [37].

Table 3
Thermodynamic parameters for Cu(II) and Zn(II) adsorption onto ACH (ACH2)

Metal ions	T(K)	ln K_c	ΔG° (kJ/mol)	ΔH° (kJ/mol)	ΔS° (J/mol K)
Cu(II)	293	1.056	–2.527	7.361	33.749
	298	1.089	–2.696		
	303	1.115	–2.865		
	308	1.173	–3.033		
	313	1.226	–3.202		
	318	1.291	–3.371		
	323	1.322	–3.540		
Zn(II)	293	0.113	–0.189	19.876	68.463
	298	0.179	–0.526		
	303	0.301	–0.862		
	308	0.492	–1.199		
	313	0.591	–1.536		
	318	0.752	–1.872		
	323	0.793	–2.209		

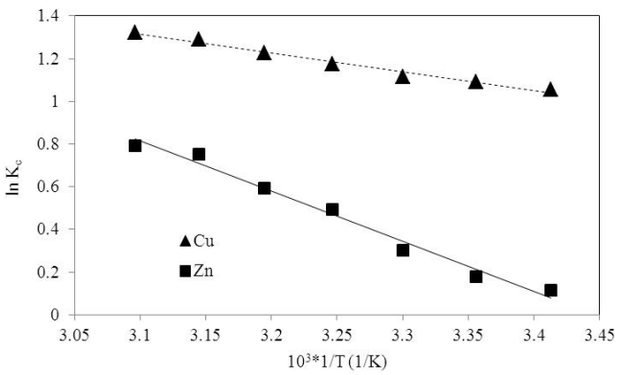

Fig. 12. Van't Hoff plot for the adsorption of Cu(II) and Zn(II) onto ACH2.

4.8. Adsorption kinetics studies

Adsorption kinetic is one of the most important method to interpret the transport of the metal ions on the solid phase for real applications and play a key role in elucidating the dominant adsorption mechanism (Fig. 13). Different kinetic models including pseudo-first-order, pseudo-second-order and were applied for the experimental data to describe the adsorption rate of an adsorbate from the liquid phase onto ACH2 [19,33]. However, the rate-limiting step were employed by Elovich and intraparticle Weber-Morris diffusion models to understand the mechanism of adsorption by ACH2 [10,38]. From Table 4, pseudo-second-order kinetics model provides a significantly better description of the kinetics of the adsorption of Cu(II) and Zn(II) ions on ACH2, suggesting a chemisorption process [39]. The Elovich equation, which applies to heterogeneous surfaces, was also applied in an effort to better describe the chemisorption process [33,40]. In the view of these results,

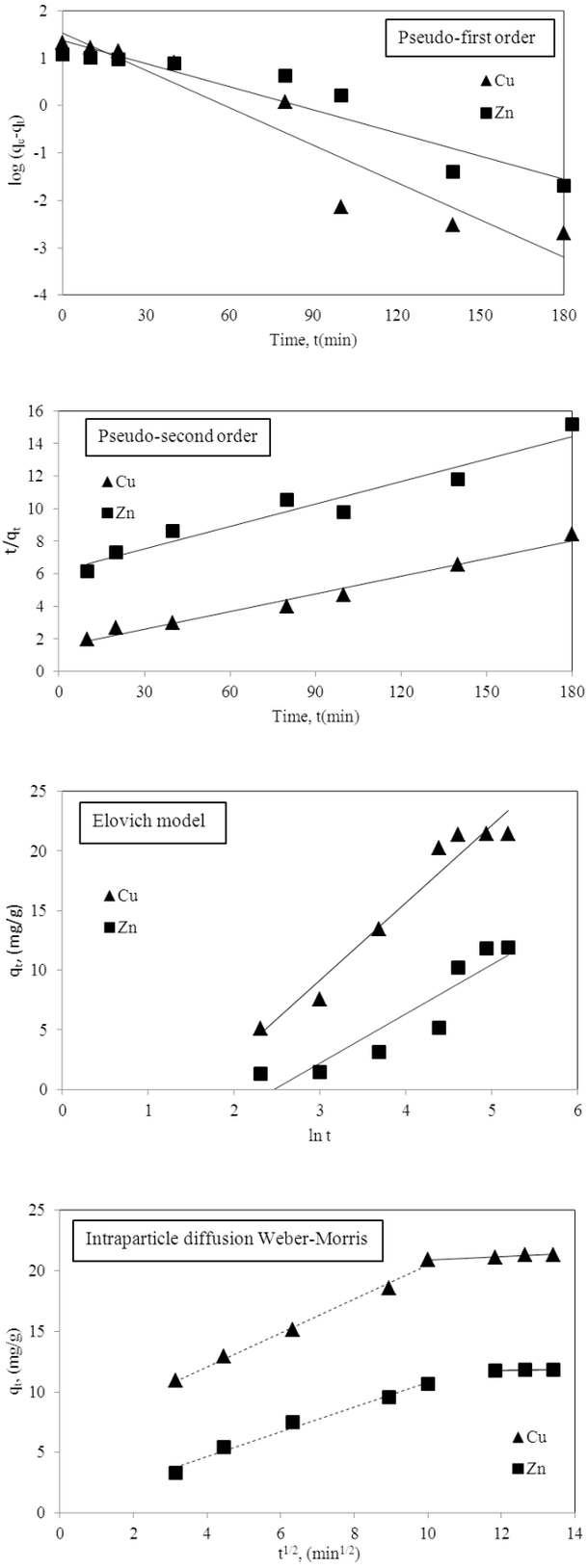

Fig. 13. Adsorption kinetics of Cu(II) and Zn(II) onto ACH2.

Table 4
Kinetic models for the adsorption of Cu(II) and Zn(II) onto ACH2

Kinetics model	Parameters	Metal ions	
		Cu(II)	Zn(II)
Pseudo-first order	q_e (mg g^{-1})	23.88	13.447
	k_1 (min^{-1})	0.06	0.037
	R^2	0.906	0.891
Pseudo-second order	$q_{e,exp}$ (mg g^{-1})	21.39	11.89
	$q_{e,cal}$ (mg g^{-1})	21.77	11.96
	$k_2 \times 10^{-3}$ (g mg^{-1} min^{-1})	0.85	0.345
	R^2	0.976	0.954
Elovich	β (mg g^{-1})	0.154	0.243
	α (mg g^{-1} min^{-1})	1.33	0.354
	R^2	0.942	0.849
Intraparticle diffusion Weber-Morris	k_{d1} (mg g^{-1} min$^{1/2}$)	1.405	1.027
	C_1 (mg g^{-1})	6.449	0.559
	R_1^2	0.994	0.984
	k_{d2} (mg g^{-1} min$^{1/2}$)	0.134	0.044
	C_2 (mg g^{-1})	19.575	11.26
	R_2^2	0.952	0.951

the correlation coefficients ($R^2 < 0.95$) obtained using the pseudo-first-order and Elovich models for adsorption of Cu(II) and Zn(II) ions on ACH2, are markedly lower than those obtained using the pseudo-second-order. In accordance with the pseudo-second-order reaction mechanism, the overall reaction kinetics for the adsorption of Cu(II) and Zn(II) onto ACH2 appear to be controlled by the chemical processes, through sharing of electrons between adsorbent and metal ions, or covalent forces, through the exchange of electrons between the particles involved [38]. However, the rate-limiting step may be either the boundary layer (film) or the intraparticle (pore) diffusion of metal ions on the surface of adsorbents in a batch process. The experimental kinetics of Cu(II) and Zn(II) Ions adsorption on ACH2 in a single component solution is characterized by a sharp increase in the adsorbed concentration during 90 min, followed by a lower uptake rate, which can be described by intraparticle Weber-Morris diffusion model in Fig. 13. The plot displays two linear portions indicating that two steps contribute to the adsorption process. The initial part is connected to faster mass transfer through the boundary layer and/or adsorption on the external surface of the adsorbent, While following part corresponds to the ongoing adsorption stage, where intraparticle diffusion is the rate-limiting step (slow diffusion inside the particles). The calculated parameters of the model are listed in Table 4. Values of intraparticle diffusion model (Table 4) give an idea about the thickness of the boundary layer, i.e., the larger the intercept, the greater is the boundary layer effect [41]. The deviation of straight lines from the origin (Fig. 13) may be because of the difference between the rate of mass transfer in the initial and final stages of adsorption. Further, such deviation of straight lines from the origin indicates that the pore diffusion is not the sole rate-controlling step [42]. The diffusion was characterized by the specific rate parameters, k_{d1} and k_{d2}. The value of k_{d1} was higher than that of k_{d2} which could be attributed to limitation of the available vacant sites for diffusion and pore blockage [43].

4.9. Adsorption isotherm studies

The adsorption isotherms revealed the specific relation between the concentration of the metal ions and its adsorption degree onto adsorbent surface at an equilibrium experiments of both single metal and binary metal system. The equilibrium adsorption isotherms were important to understand the mechanism of the adsorption. Several isotherm equations were available and three adsorption isotherm models (Langmuir, Freundlich and Temkin) were used in the present study. To quantify the adsorption capacity of ACH for the removal of Cu(II) and Zn(II) ions from aqueous solution, the Langmuir, Freundlich and Temkin isotherm models were the most frequently used simple isotherm describing the equilibrium [44]. Data fitted with Langmuir, Freundlich and Temkin isotherm models are given in Table 5 and Figs. 14–16. The Langmuir isotherm model indicates the formation of monolayer coverage of heavy metal ions on the outer surface of adsorbent. The Langmuir equation is based on the assumption that intermolecular forces decrease rapidly with distance and monolayer adsorption occurred on the outer surface of sorbent, in which all adsorption sites are homogeneous [45]. The maximum adsorption capacity of Cu(II) and Zn(II) ions obtained from Langmuir isotherm experiments is 29.41 and 14.64 mg g^{-1}, respectively. The maximum adsorption capacity to form a monolayer is found higher in case of comparing with the constant (q_m, mg g^{-1}), which is a measure from the adsorption study of activated carbon derived from *Hevea brasiliensis* [46], the adsorption efficiency in this study is much higher. The Freundlich isotherm model is employed to describe the adsorption on heterogeneous surface which is not restricted to the formation of monolayer and the fractional values of $1/n$, from Freundlich isotherm model (Table 5), suggests the heterogeneity of adsorbent surface and simultaneously indicated a favorable adsorption of metal ions. The higher R^2 value suggests that the Freundlich isotherm describes the adsorption process well as compare to Langmuir isotherm model for single system. The correlation coefficients (R^2) value obtains in case of Freundlich isotherm is 0.995 for Cu(II) and that value is 0.987 for Zn (II) and in case of Langmuir isotherm model both R^2 values are considerably lower versus Freundlich isotherm. The higher R^2 value suggests that the Freundlich isotherm describes the adsorption process well as compare to Langmuir isotherm model for both metal ions. The essential feature of the Freundlich isotherm can be expressed by 'n', referred to as intensity factors. As the values of $n > 1$ represent favorable adsorption condition [47]. The n values in this study are 1,633 and 1,637 mg/g for Cu(II) and Zn(II) ions, respectively, which indicate that Freundlich isotherm is considered to be adequate for describing the adsorption of both metals on ACH2, with a somewhat better fit at the higher concentration of metal ions. The Temkin adsorption potential (K_T), of ACH2 for Cu(II) and Zn(II) are 0.311 and 0.411 respectively, indicating a lower ACH2 -metal ions potential for Cu(II) probably due to its small ionic radius. The Temkin constant, b_T, related to

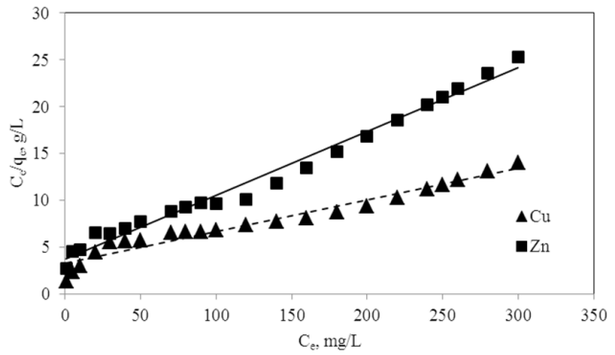

Fig. 14. Langmuir isotherm for the adsorption of Cu(II) and Zn(II) onto ACH2.

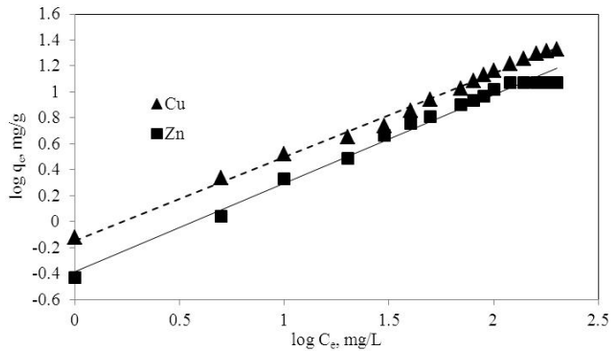

Fig. 15. Freundlich isotherm for the adsorption of Cu(II) and Zn(II) onto ACH2.

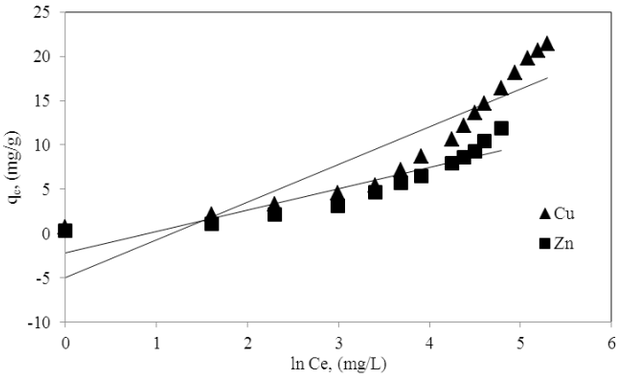

Fig. 16. Temkin isotherm for the adsorption of Cu(II) and Zn(II) onto ACH2.

heat of sorption for the two metal ions were 0.613 and 1.082 kJ mol^{-1} for Cu (II) and Zn(II) respectively. The values of b_T obtained in this study indicate that the adsorption process seemed to be involved in the chemical sorption [48].In terms of R^2 values, the applicability of the above three models for present experimental data approximately followed the order: Freundlich > Langmuir > Temkin can conclude from (R^2) values that Freundlich isotherm is the best followed by the other isotherms.

Table 5
Adsorption isotherm constants for Cu(II) and Zn(II) adsorption on ACH2

Equilibrium model	Parameters	Metal ions	
		Cu(II)	Zn(II)
Langmuir isotherm	q_m (mg g^{-1})	29.41	14.64
	K_a (L mg^{-1})	0.0105	0.0186
	R_L	0.323	0.309
	R^2	0.951	0.964
Freundlich isotherm	K_f (mg g^{-1})	0.721	0.410
	n (mg g^{-1})	1.633	1.637
	R^2	0.995	0.987
Temkin isotherm	K_T	0.311	0.411
	B_T (mg g^{-1})	4.245	2.405
	b_T (kJ mol^{-1})	0.613	1.082
	R^2	0.812	0.843

4.10. Comparison of ACH with other adsorbents

Based on previous relevant studies, the amount of heavy metals adsorbed by various materials of activated carbon was highly variable (Table 6). In the current study, activated carbon derived from Halophytes (*Suaeda maritime*) demonstrated an enhanced removal efficiency when compared with other adsorbents. Rajaei et al. [49] mentioned that the removal efficiency was dependent upon the physico-chemical characteristics of the adsorbent and the metal removed, which was the case of the activated carbon samples. In this study, R^2 values for the Freundlich isotherm model were higher than those for the Langmuir isotherm model. This indicated that the Freundlich model better described the adsorption of both metal ions onto ACH2, with a confirming the tight relationship between the physicochemical properties of the adsorbent and its removal capacity. These results indicated much

Table 6
Comparison of adsorption capacity for various kinds of activated carbon

Adsorbent	Adsorption capacity (mg/g)		References
	Cu(II)	Zn(II)	
Halophytes (Suaeda maritime, ACH2)	29.41	14.64	Present study
Modified fir tree sawdust	12.7	13.4	[50]
Modified poplar tree sawdust	6.92	15.8	[50]
Vitex doniana Nut	–	2.356	[51]
Crude olive stone	–	20.52	[52]
Typha latifolia L.	28.8	9.9	[49]
Populous deltoids leaves	17.76	–	[53]
Syzygium cumini leaves	15.87	–	[53]
Durian tree sawdust	18.42	22.78	[54]
Oil palm empty fruit bunch	26.95	21.19	[54]

higher removal efficiency for ACH2 than that shown by Song et al. [1] who reviewed the removal of metals like copper(II), cadmium(II), and zinc(II) by various kinds of activated carbon (Table 6). Therefore, the activated carbon derived from Halophytes (*Suaeda maritime*) which collected from northern Egypt exhibited greater removal efficiency than other adsorbents, confirming their beneficial use for the removal Cu(II) and Zn(II) from aqueous solutions.

5. Conclusion

This study investigated the feasibility of activated carbon derived from Halophytes used as an inexpensive adsorbent for the removal of Cu(II) and Zn (II) from aqueous solution. The adsorption process was observed to be greatly dependent on pH value, adsorption time, dose of ACH2, temperature and the initial concentration of metal ions. Thermodynamics studies indicated that the adsorption is natively spontaneous and endothermic. The adsorption kinetic for ACH2 was well described by the chemisorption model of pseudo-second-order kinetics. The experimental results were analyzed using four adsorption isotherm models, the Langmuir, Freundlich and Temkin, isotherm models. Furthermore, it was proved that adsorption of Cu(II) and Zn (II) ions ACH2 have experimental data obtained correspond to Freundlich isotherm model. Consequently, the yield of activated carbon from Halophytes by phosphoric acid activation can be used as adsorbents for various environmental applications including treatment of drinking water and removal of heavy metals from industrial effluents.

Acknowledgement

Both authors would like to thank the staff of Central Laboratory for Environmental Quality Monitoring for their cooperation during measurements for providing necessary facilities to accomplish the work. Special thanks devoted to Central Laboratory for Tanta University to support present research and the required devices.

References

[1] J. Song, R. Zhang, K. Li, B. Li, C. Tang, Adsorption of copper and zinc on activated carbon prepared from Typha latifolia L, Clean – Soil Air Water., 43(2015) 79–85.
[2] R.S. Ayers, D.W. Westcot, Water quality for agriculture, FAO irrigation and drainage paper 29 rev 1. FAO, UN, Rome, (1985) 174–187.
[3] M. Dou, J. Ma, G. Li, Q. Zuo, Measurement and assessment of water resources carrying capacity in Henan Province, China, Water Sci Eng., 8 (2015) 102–113.
[4] C.N. Mulligan, R.N. Yong, B.F. Gibbs, Remediation technologies for metal-contaminated soils and groundwater: an evaluation, Eng. Geol., 60 (2001) 193–207.
[5] J. Yoon, X. Cao, Q. Zhou, L.Q. Ma, Accumulation of Pb, Cu, and Zn in native plants growing on a contaminated Florida site, Sci. Total. Environ., 368 (2006) 456–464.
[6] A. Hawari, Z. Rawajfih, N. Nsour, Equilibrium and thermodynamic analysis of zinc ions adsorption by olive oil mill solid residues, J. Hazard. Mater., 168 (2009) 1284–1289.
[7] M.A. Ferro-Garcia, J. Rivera-Utrilla, J. Rodrfguez-Gordillo, I. Bautista-Toledo, Adsorption of zinc, cadmium, and copper on activated carbons obtained from agricultural by-products, Carbon, 26 (1986) 363–373.
[8] B. Saha, M.H. Tai, M. Streat, Metal sorption performance of an activated carbon after oxidation and subsequent treatment, Process Saf. Environ Prot., 79 (2001) 345–351.
[9] L.C. Romero, A. Bonomo, E.E. Gonzo, Peanut shell activated carbon: adsorption capacities for copper(II), zinc(II), nickel(II) and chromium(VI) ions from aqueous solutions, Adsorpt. Sci. Technol., 22 (2004) 237–243.
[10] F. Bouhamed, Z. Elouear, J. Bouzid, B. Ouddane, Multi-component adsorption of copper, nickel and zinc from aqueous solutions onto activated carbon prepared from date stones, Environ. Sci. Pollut. Res., 23 (2016) 15801–15806.
[11] H.M. El Shaer, Halophytes and salttolerant plants as potential forage for ruminants in the Near East region, Small Ruminant Res., 91 (2010) 3–12.
[12] N. Atar, A. Olgun, S. Wangb, Adsorption of cadmium (II) and zinc (II) on boron enrichment process waste in aqueous solution: batch and fixed system studies, Chem. Eng. J., 192 (2012) 1–7.
[13] S. Madhavakrishnan, K. Manicckavasagam, K. Rasappan, P.S. Syed Shabudeen, R. Venkatesh, S. Pattabhi, Ricinus communis pericarp activated carbon used as an adsorbent for the removal of Ni(II) from aqueous solution, J. Chem., 5 (2008) 761–769.
[14] P. Abdul Latif, B.H. Guan, T.H. Yap, Physical preparation of activated carbon from sugarcane bagasse and corn husk and its physical and chemical characteristics, Int. J. Eng. Res. Sci. Tech., 2 (2013) 1–14.
[15] S.M. Anisuzzaman, C.G. Joseph, Y.H. Taufiq-Yap, D. Krishnaiah, V.V. Tay, Modification of commercial activated carbon for the removal of 2,4-dichlorophenol from simulated wastewater, J. K. Saud Univ-Sci., 27 (2015) 318–330.
[16] K.S.W. Sing, D.H. Everett, R.A.W. Haul, L. Moscou, R.A. Pierotti, J. Rouquerol, T. Siemieniewska, Reporting physisorption data for gas/solid systems with special reference to the determination of surface area and porosity, Pure Appl. Chem., 57 (1985) 603–619.
[17] L.Y. Hsu, H. Teng, Influence of different chemical reagents on the preparation of activated carbons from bituminous coal, Fuel Process. Technol., 64 (2000) 155–166.
[18] S.M. Yakout, G. Sharaf El-Deen, Characterization of activated carbon prepared by phosphoric acid activation of olive stones, Arab J. Chem., 9 (2016) 1155–1162.
[19] Y.S. Ho, G. McKay, Kinetic models for the sorption of dye from aqueous solution by wood, J. Environ. Sci. Health Part B., 76 (1998) 183–191.
[20] N. Fiol, I. Villaescusa, Determination of sorbent point zero charge: usefulness in sorption studies, Environ. Chem. Lett., 7 (2005) 79–84.
[21] G. Tian, W. Wang, Y. Kang, A. Wang, Ammonium sulfide-assisted hydrothermal activation of palygorskite for enhanced adsorption of methyl violet, J. Environ. Sci., 41 (2016) 33–43.
[22] S. Qaiser, R. Anwar, U. Muhammad, Biosorption of lead (II) and chromium(VI) on groundnut hull: Equilibrium, kinetics and thermodynamics study, Electron. J. Biotechnol., 12 (2009) 1–4.
[23] Y.B. Onundi, A.A. Mamun, M.F. Al Khatib, Y.M. Ahmed, Adsorption of copper, nickel and lead ions from synthetic semiconductor industrial wastewater by palm shell activated carbon, Inter. J. Environ. Sci. Technol., 7 (2010) 751–758.
[24] K.Y. Foo, B.H. Hameed, Utrilization of biodiesel waste as a renewable resource for activated carbon: Application to environmental problems, Renew. Sust. Energ. Rev., 13 (2009) 2495–2504.
[25] A.M. Puziy, O.I. Poddubnaya, A. Martınez-Alonso, F. Suarez-Garcıa, J.M.D. Tascon, Synthetic carbons activated with phosphoric acid I. Surface chemistry and ion binding properties, Carbon, 40 (2002) 1493–1505.

[26] T. Budinova, E. Ekinci, F. Yardim, A. Grimm, E. Bjornbom, V. Minkova, M. Goranova, Characterization and application of activates carbon produced by $H_3PO_4$and water vapor activation, Fuel Process Technol., 87 (2006) 899–905.
[27] M.A. Hubbe, S.H. Hasan, J.J. Ducoste, Metal ion sorption: Review. Bioresour., 6 (2011) 2161–2287.
[28] M. Rafatullah, O. Sulaiman, R. Hashim, A. Ahmad, Adsorption of Copper(II) onto Different Adsorbents, J. Dispers. Sci. Technol., 31 (2010) 918–930.
[29] G .Chen, J. Fan, R. Liu, G. Zeng, A. Chen, Z. Zou, Removal of Cd(II), Cu(II) and Zn(II) from aqueous solutions by live Phanerochaete Chrysosporium, Environ. Technol., 33 (2012) 2653–2659.
[30] L. Monser, N. Adhum, Modified activated carbon for the removal of copper, zinc, chromium and cyanide from wastewater, Sep. Purif. Technol., 26 (2002) 137–146.
[31] O. Hamdaoui, Batch study of liquid-phase adsorption of methylene blue using cedar sawdust and crushed brick, J. Hazard. Mater., 135 (2006) 264–273.
[32] D. Ozdes, A. Gundogdu, B. Kemer, C. Duran, H.B. Senturk, M. Soylak, R.M. Suzuki, Removal of Pb(II) ions from aqueous solution by a waste mud from copper mine industry: equilibrium, kinetic and thermodynamic study, J. Hazard. Mater., 166 (2009) 1480–1487.
[33] E. Sočo, J. Kalembkiewicz, Removal of copper(II) and zinc(II) ions from aqueous solution by chemical treatment of coal fly ash, Croat. Chem. Acta., 88 (2015) 267–279.
[34] J.K. Oubagaranadin, Z.P. Murthy, Z.P. Mallapur, Removal of Cu(II) and Zn(II) from industrial wastewater by acid–activated montmorillonite-illite type of clay, Comptes Rendus Chimie., 13 (2010) 1359–1363.
[35] S.H. Guo, W. Li, L.B. Zhang, J.H. Peng, H.Y. Xia, S.M. Zhang, Kinetics and equilibrium adsorption study of lead(II) onto the low cost adsorbent – Eupatorium adenophorumSpreng, Process Saf. Environ. Prot., 87 (2009) 343–351.
[36] D. Mohan, K.P. Singh, Single- and multi-component adsorption of cadmium and zinc using activated carbon derived from bagasse – an agricultural waste, Water Res., 36 (2002) 2304–2318.
[37] A.T. Sdiri, T. Higashi, F. Jamoussi, Adsorption of copper and zinc onto natural clay in single and binary systems, Int. J. Environ. Sci. Technol., 11 (2014) 1081–1092.
[38] X.C. Chen, G.G. Chen, L.G. Chen, Y.X. Chen, J. Lehmann, M.B. McBride, A.G. Hay, Adsorption of copper and zinc by biochars produced from pyrolysis of hardwood and corn straw in aqueous solution, Bioresour. Technol., 102 (2011) 8877–8884.
[39] Y.S. Ho, Effect of pH on lead removal from water using tree fern as the sorbent, Bioresour. Technol., 96 (2005) 1292–1296.
[40] X.S. Wang, Z.Z. Li, S.R. Tao, Removal of chromium (VI) from aqueous solution using walnut hull, J. Environ. Manage., 90 (2009) 721–729.
[41] M.A. Wahab, H. Boubakri, S. Jellali, N. Jedidi, Characterization of ammonium retention processes onto cactus leaves fibers using FTIR, EDX and SEM analysis, J. Hazard. Mater., 241–242 (2012) 101–109.
[42] M.A. Ahmad, N. Azreen A. Puad, O. Bello, Kinetic, equilibrium and thermodynamic studies of synthetic dye removal using pomegranate peel activated carbon prepared by microwave-induced KOH activation, Water Resour. Indust., 6 (2014) 18–35.
[43] E. Demirbas, M. Kobya, M.T. Sulak, Adsorption kinetics of a basic dye from aqueous solutions onto apricot stone activated carbon, Biores. Technol., 99 (2008) 5368–5373.
[44] F. Chigondo, B.C. Nyamunda, S.C. Sithole, L. Gwatidzo, Removal of lead (II) and copper (II) ions from aqueous solution by baobab (*Adononsia digitata*) fruit shells biomass, J. Appl. Chem., 5 (2013) 43–50.
[45] M.S. Mansour, M.E. Ossman, H.A. Farag, Removal of Cd (II) ion from waste water by adsorption onto polyaniline coated on sawdust, Desalination, 272 (2011) 301–305.
[46] N. Sivarajasekar, Hevea brasiliensis – A Biosorbent for the adsorption of Cu(II) from aqueous solutions, Carbon Lett., 8 (2007) 199–206.
[47] S. Pandey, S.B. Mishra, Organic–inorganic hybrid of chitosan/organoclay bionanocomposites for hexavalent chromium uptake, J. Coll. Interface Sci., 361 (2011) 509–520.
[48] A. Cinnoti, N. Lai, R. Orru, G. Cao, Sardain natural clinoptilolites for heavy metals and ammonium removal: experimental and modelling, Chem. Eng. J., 84 (2001) 275–282.
[49] G.E. Rajaei, H. Aghaie, K. Zare, M. Aghaie, Adsorption of Cu(II) and Zn(II) ions from aqueous solutions onto fine powder of Typha latifolia L. root: kinetics and isotherm studies, Res. Chem. Intermed., 39 (2013) 3579–3594.
[50] M. Šćiban, M. Klašnja, B. Škrbić, Modified softwood sawdust as adsorbent of heavy metal ions from water, J. Hazard. Mater., 136 (2006) 266–271.
[51] P.O. Ameh, R. Odoh, A. Oluwaseye, Equilibrium study on the adsorption of Zn(II) and Pb(II) ions from aqueous solution onto Vitex doniana nut, Int. J. Modern Chem., 3 (2012) 82–97.
[52] U. Kouakou, A.S. Ello, J.A. Yapo, A. Trokourey, Adsorption of iron and zinc on commercial activated carbon, J. Environ. Chem. Ecotoxicol., 5 (2013) 168–171.
[53] R. Kaur, J. Singh, R. Khare, S.S. Cameotra, A. Ali, Batch sorption dynamics, kinetics and equilibrium studies of Cr(VI), Ni(II) and Cu(II) from aqueous phase using agricultural residues, Appl. Water Sci., 3 (2013) 207–218.
[54] S.M. Yusoff, A. Kamari, W.P. Putra, C.F. Ishak, A. Mohamed, N. Hashim, I.M. Isa, Removal of Cu(II), Pb(II) and Zn(II) ions from aqueous solutions using selected agricultural wastes: adsorption and characterization studies, J. Environ. Prot., 5 (2014) 289–300.